

Structure and Properties of Regenerated Cellulose Filaments Prepared from Cellulose Carbamate–NaOH/ZnO Aqueous Solution

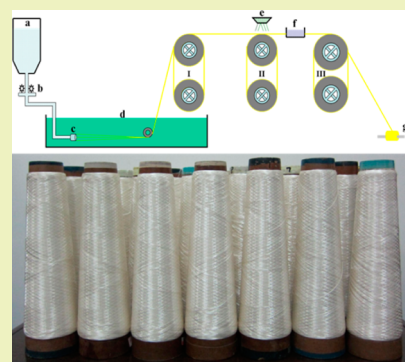
Feiya Fu,[†] Quanling Yang,[‡] Jinping Zhou,^{*,†} Haoze Hu,[†] Baoquan Jia,[†] and Lina Zhang[†]

[†]Department of Chemistry and Key Laboratory of Biomedical Polymers of Ministry of Education, Wuhan University, Wuhan 430072, China

[‡]Graduate School of Agricultural and Life Sciences, The University of Tokyo, 1-1-1 Yayoi, Bunkyo-ku, Tokyo 113-8657, Japan

ABSTRACT: In this work, regenerated cellulose (RC) filaments were successfully spun from cellulose carbamate in a NaOH/ZnO aqueous solution on a pilot scale. The structure and properties of the RC filaments were characterized using SEM, FT-IR, elemental analysis, ¹³C NMR, XRD, 2D WAXD, tensile testing, and dye testing. The nitrogen-free and sulfur-free RC filaments exhibited a bright surface and circular cross section. The filaments demonstrated a typical cellulose II crystal structure and a relatively high degree of orientation. Improved tenacity and structure were obtained in the RC fibers due to improved post-processing spinning steps and an increased drawing ratio. The tenacity of the fibers was determined in the range of 1.69–2.36 cN/dtex, which was comparable with that of commercial viscose rayon. Furthermore, the RC filaments showed improved dye properties compared with viscose rayon. The described carbamate pathway provided a simple and environmentally friendly method, offering an alternate to the environmental drawbacks of the viscose process.

KEYWORDS: Cellulose filaments, Cellulose carbamate, Orientation, Mechanical properties, Dye properties



INTRODUCTION

As a widely abundant renewable organic material, cellulose exhibits outstanding properties and useful applications but also presents challenges due to economic and environmental issues in chemical processing.^{1,2} The traditional viscose method for regenerated cellulose (RC) fiber (viscose rayon) is well over 100 years old but remains the dominant method.^{3,4} Viscose rayon is produced today worldwide on a 5 million ton scale, and its types range from high performance tire yarn to textile filaments and staple fibers with excellent properties close to those of cotton.⁵ However, residual sulfates (8 mg/100 g multifilament) in viscose rayon limited its application in some fields.⁶ Increasing concerns over the environmental consequences of viscose production has led to the closure of viscose production plants in most developed countries.^{3,6} The development of new environmentally friendly spinning systems for RC production is thus highly valuable. At the end of the last century, new processing technology was proposed using a more environmentally friendly solvent known as N-methylmorpholine-N-oxide (NMMO); this solvent provided a new class of man-made cellulose fibers, which were commercialized by the Lenzing Group under the generic name of Lyocell.^{7,8} Compared with conventional viscose rayon, Lyocell fibers have outstanding properties in many respects, such as strength in both wet and dry states, modulus of elasticity, sorption behavior, wearing properties, gloss, and touch.^{3,7,8} More recently, room-temperature ionic liquids (ILs) have been identified as effective and promising cellulose solvents with desirable green properties.^{9,10} There are a few reports on the spinning of cellulose/IL solutions, and the obtained RC fiber is

named Ionicell.^{11–13} The Thuringian Institute of Textile and Plastic Research has studied the dissolution of cellulose in different ILs and prepared RC fibers by a dry–wet-spinning process.¹⁴ The Institute for Textile Chemistry and Chemical Fibers manufactured RC fibers by a wet-spinning process using 1-ethyl-3-methylimidazolium acetate as the direct solvent. The resultant Ionicell fibers demonstrated a smooth surface, round and compact structure, and dye and antifibrillation properties similar to those seen in Lyocell fibers.^{11,13} A series of water-based solvent systems for cellulose have also been reported. It was found that cellulose could be dissolved quickly in any of the precooled aqueous solutions of NaOH/urea,¹⁵ NaOH/thiourea,¹⁶ or NaOH/thiourea/urea.¹⁷ Initial studies examined the properties of these cellulose solutions and their resulting fibers; advantages were established in the inexpensiveness and low toxic effects of the solvent systems.^{6,18–22} The development of a novel process that could utilize existing viscose production plants would be of great significance in the cellulose industry. However, the aforementioned spinning processes exhibit significant differences from the existing viscose process, and a number of disadvantages are thus presented in solvent recovery and spinning dope stability.³ Novel spinning processes still require extensive development, with a particular need to confront key challenges in high power consumption and equipment costs before the process can be applied to industrial production on a large scale.

Received: August 27, 2014

Revised: September 15, 2014

Published: September 17, 2014

On the other hand, the cellulose carbamate (CC) process, a method first developed by the well-known viscose fiber manufacturers Kemira Oy Saeteri and Neste Oy, can utilize traditional viscose spinning technology.^{5,23,24} The CarbaCell process is a specific carbamate technology using a novel synthesis route for CC with xylene as the transfer medium.⁵ The obtained CC is soluble in NaOH aqueous solution. The CC solution can then be spun into a diluted acidic or sodium carbonate using a regenerating bath to form fibers. The carbamate fibers exhibit similar properties to viscose rayon. CC is also advantageous due to its relatively high stability at room temperature, which allows storage for over a year.^{23,24} However, some hard conditions including catalysts, organic solvents, long reaction time, and high temperature are not favored for the scale up of the carbamate technology, and it is not yet to be applied in industrial use.^{25–28} In our previous work, a novel process was presented for the synthesis of CC using microwave heating under catalyst-free and solvent-free conditions.^{29,30} The process decreased reaction time from hours to minutes, which was greatly significant for the commercialization of the carbamate process. Most recently, it was determined that the solubility of CC could be significantly improved with the addition of a small amount of ZnO to the NaOH solution.³¹ Moreover, green methods for the production of cellulose multifilament and membranes from CC have been reported.^{31,32} The lower cost and lower toxicity of our novel carbamate method, and its relative ease for wet spinning, exhibited some good promises for the development of a more economic and environmentally friendly process for regeneration of RC fibers. The spinning conditions are hugely influential in cellulose regeneration. Herein, we attempt to prepare RC multifilaments from a CC solution using a pilot machine and to study the post-processing spinning steps and drawing process in terms of the structure and properties of the obtained filaments.

EXPERIMENTAL SECTION

Materials. Cotton linter pulp with an α -cellulose content of more than 93% and viscose rayon were provided by the Hubei Chemical Fiber Group Ltd. (Xiangyang, China). The degree of polymerization (DP) of the cellulose and viscose rayon samples were determined to be 784 and 371, respectively. Commercially available urea was utilized for microwave synthesis of CC. All other chemical reagents were of analytical grade and were purchased from commercial producers in China.

Microwave Synthesis of CC. CC samples were prepared in accordance with the previous work.^{29,30} Cellulose was immersed into a 45 wt % urea aqueous solution. The mixture then stood at ambient temperature for 3 h, followed by dehydration separation and oven drying. The obtained mixture of cellulose/urea was subsequently heated in a microwave oven (Whirlpool, VIP 273F, 850 W, 10 levels) at 425 W for 12 min. Finally, the sample was washed with water and vacuum-dried. The obtained CC sample was obtained with a DP of 623. The nitrogen content (N%) and degree of substitution (DS) of the CC samples were 2.089% and 0.26, respectively.

Dissolution of CC and Wet Spinning. In accordance with the previous work,³² an aqueous solution was prepared for the CC solvent by directly mixing NaOH, ZnO and distilled water (7:1.6:81.4 in wt %). Then, the desired amount of CC sample was dispersed into the solvent system (9 L) and cooled to -12 °C to obtain a transparent CC dope (5.5 wt %). The resultant CC dope was filtered through 350 pore meshes and degassed in a vacuum oven (-0.09 MPa) for 8 h at ambient temperature.

The wet-spinning process was carried out on a preliminary pilot apparatus that was constructed by Hubei Chemical Fiber Co. Ltd. (Xiangyang, China). The schematic diagram of this apparatus is shown

in Scheme 1, and the wet spinning parameters are listed in Table 1. The spinneret cylinder (75 orifices; diameter, 80 μ m) was directly

Scheme 1. Schematic Diagram of the Pilot Scale Spinning Machine: (a) Stainless Steel Reservoir, (b) Metering Pump, (c) Spinneret, (d) Coagulation Bath, (e) Hot Water Washing, (f) Plasticizing Bath, and (g) Take-Up Roller; (I) Nelson-Type Roller, (II) Nelson-Type Roller, and (III) Heating Roller

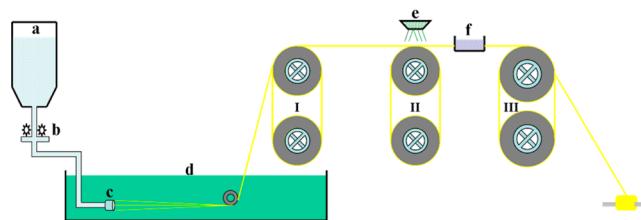


Table 1. Wet-Spinning Parameters of RC Filaments from Cellulose Carbamate–NaOH/ZnO Aqueous Solution

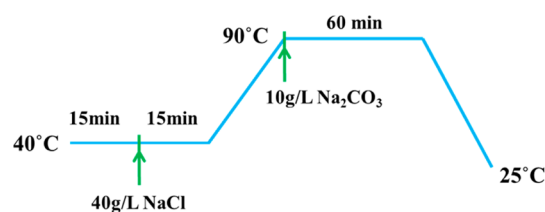
sample	flow speed at spinneret (m/min)	v_I (m/min) SDR _I	v_{II} (m/min) SDR _{II}	v_{III} (m/min) SDR _{III}
RCF-1	60	30/0.50	31/1.03	32/1.03
RCF-2	60	36/0.60	37/1.03	38/1.03
RCF-3	60	41/0.68	42/1.02	43/1.02
RCF-4	60	45/0.75	46/1.02	46/1.00
RCF-5	60	49/0.82	49/1.00	50/1.02

v_I , v_{II} , and v_{III} are the spinning speed of Nelson-type rollers I and II and the heating roller, respectively. SDR_I, SDR_{II}, and SDR_{III} are the spinning drawing ratio of Nelson-type rollers I and II and the heating roller, respectively.

immersed into a coagulation bath of 8 wt % H₂SO₄/20 wt % Na₂SO₄ solution at 25 °C. The resultant gelation fibers were taken up on the Nelson-type roller I and then drawn to the Nelson-type roller II. The residual salts and acids were washed out by placing the resultant multifilament fibers in a water bath at 45 °C until the pH of the fibers was about 7, before plasticization. Finally, the fibers were dried using a heating roller (surface temperature, 75 °C) and wound on a spool to obtain multifilament fibers. With an increase in the drawing ratio on the Nelson-type roller I, RC fibers were collected on the take-up roller and were coded as RCF-1, RCF-2, RCF-3, RCF-4, and RCF-5. RC fibers were gathered at each spinning stage from the Nelson-type rollers I and II and take-up roller and coded as RCF-4-I, RCF-4-II, and RCF-4, respectively.

Dye Testing. Three reactive dyes of commercial grade, namely, KE-3B (C.I. Reactive Red 120), KE-4R (C.I. Reactive Yellow 84), and KE-2B (C.I. Reactive Blue 160), were used without purification. A 250 mL dye bath containing a reactive dye (3.0% o.w.f) was prepared, which was deemed suitable for a 1.0 g sample of rayon (liquor ratio 1:50). The employed dyeing method used is shown in Scheme 2. Fabric was first dyed with the reactive dyes and then treated with a

Scheme 2. Reactive Dyeing Profile for Novel RC Filaments and Commercial Viscose Rayon



soaping agent (2 g/L) for 10 min at 95 °C. The dye exhaustion ratio (E) was calculated as follows¹¹

$$X = \frac{A_b}{A_a \times n} \times 100\% \quad (1)$$

$$E = 100\% - X \quad (2)$$

where X is the dye content in the residual dye solution, A_a is the absorbance value of the standard dye solution, A_b is the absorbance value of the residual dye solution, and n is the ratio of the concentration (g/L) of the standard dye solution to the residual dye solution. The dye fixing ratio (F) was obtained in accordance with the following equation¹¹

$$Y = \frac{A_d}{A_c \times n} \times 100\% \quad (3)$$

$$F = E - Y \quad (4)$$

where Y is the unfixed dye content in the residual soaping solution, A_c is the absorbance value of the standard soaping solution, A_d is the absorbance value of the residual soaping solution, and n is the ratio of the concentration (g/L) of the standard soaping solution to the residual soaping solution.

All of the absorbance values were measured with a UV-3000 spectrophotometer (Shimadzu, Kyoto, Japan). Higher dye exhaustion ratios and dye fixing ratios were associated with better dye properties in the fibers. The dye quality of the RC fibers and viscose rayon was evaluated using a color yield parameter. The color strength (K/S) of the dyed samples was carried out on a Datacolor SF600 computer color matching system (Datacolor International, U.S.A.).

Characterization. The viscosity of the samples was measured in cadoxen at 25 °C, and DP was calculated from the intrinsic viscosity ($[\eta]$) in accordance with the following Mark–Houwink equation³³

$$[\eta] = 1.75 \times DP^{0.69} (\text{mL/g}) \quad (5)$$

The nitrogen and sulfur content of the CC and RC fibers were determined using an elemental analyzer (CHN-O-RAPID Heraeus Co., Germany). FT-IR spectra were determined on a FTIR spectrometer (NICOLET 5700, Thermo Electron Co., U.S.A.). The test specimens were prepared through the KBr-disk method using a reflection method. The samples were ground into powders and then vacuum-dried for 24 h before measurement. Solid state ¹³C NMR spectra were recorded on an Infinity Plus 400 spectrometer (Varian, U.S.A., magnetic field = 9.4 T, ¹³C frequency = 100.12 MHz) with a CP/MAS unit at room temperature. The spinning rate and contact time were 5.0 kHz and 5.0 ms, respectively. The pulse width, spectral width, and acquisition time were 2.10 μs, 50.0 kHz, and 20.48 ms, respectively; 2000 scans were accumulated for each spectrum. The CH signal of 6-methylbenzene was used as an external reference for the determination of chemical shifts.

X-ray diffraction (XRD) measurements of the RC fibers and CC samples were performed in reflection mode on an X-ray diffractometer (D8-Advance, Bruker, Germany). The samples were ground into powders to eliminate influences from crystalline orientation. The patterns with Cu K α radiation ($\lambda = 0.15406$ nm) at 40 kV and 30 mA were recorded in the region of 2θ from 6° to 40°. The degree of crystallinity (χ_c) was calculated by³⁴

$$\chi_c = F_c / (F_c + F_a) \times 100\% \quad (6)$$

where F_c and F_a are the areas of the crystal and amorphous regions, respectively.

Two-dimensional wide-angle X-ray diffraction (2D WAXD) measurements of the RC fibers were performed on a WAXD diffractometer (D/MAX-1200, Rigaku Denki, Japan). The typical collection time was 2 h. Two kinds of orientation factors were calculated from the 020 equatorial reflection azimuthal intensity distribution graphs (most intense peak), namely, the degree of orientation (Π) and Hermans' orientation parameter (f), in accordance with eqs 7–9.³⁵ f describes the orientation of the cellulose

crystallites axis relative to other axes of interest (herein: the axis of drawing). $fwhm$ represents the full width at half-maximum, φ represents the azimuthal angle (angle between the axis of drawing and cellulose crystallites axis), and $I(\varphi)$ represents the intensity along the Debye–Scherrer ring. $f = 1$ corresponds to the maximum orientation parallel to the drawing direction, whereas $f = 0$ indicates random orientation in the fibrils.

$$\Pi = \frac{180 - fwhm}{180} \quad (7)$$

$$f = \frac{3\langle \cos^2 \varphi \rangle - 1}{2} \quad (8)$$

$$\langle \cos^2 \varphi \rangle = \frac{\sum_0^{\pi/2} I(\varphi) \sin \varphi \cos^2 \varphi}{\sum_0^{\pi/2} I(\varphi) \sin \varphi} \quad (9)$$

The surface and cross section of the RC fibers were observed using a scanning electron microscope (VEGA 3 LMU, TESCAN, Czech). The fibers were frozen in liquid nitrogen, immediately snapped, and then vacuum-dried. The surface and the fracture surface (cross section) of the fibers were sputtered with gold and then observed and photographed. The cross section of the RC filaments was observed on an optical polarizing microscope (Leica DMLP, Germany). A bundle of fibers was embedded in celloidin and left to harden for approximately 5 min at 25 °C. Cross sections of the fiber axis of about 2 mm thickness were prepared using a Struers Accutom. The cross sections were ground and polished down to a thickness between 10 and 40 μm and then cemented to a microscope glass slide with glycerol.

The thickness of the fibers (linear density) was calculated in terms of denier, defined as the weight in grams per 9000 m of the fiber. The capability of the fibers for moisture recovery and shrinkage in boiling water was calculated in accordance with the National Standards of China (GBT13758-2008).⁴⁰ The tenacity (σ_b) and elongation at break (ϵ_b) of the filaments were measured on a universal tensile tester (XQ-1, Shanghai Textile University, China) in accordance with the ASTM method D2256-80. The σ_b and ϵ_b values were obtained at an average of 20 measurements.

RESULTS AND DISCUSSION

Morphology of RC Filaments. Multifilament fibers were successfully spun through a new carbamate pathway on a preliminary pilot-scale machine using an efficient microwave synthesis and powerful NaOH/ZnO solvent system. A photograph of the RC filaments is displayed in Figure 1. The



Figure 1. Photograph of the novel RC multifilament produced by a pilot machine from cellulose carbamate.

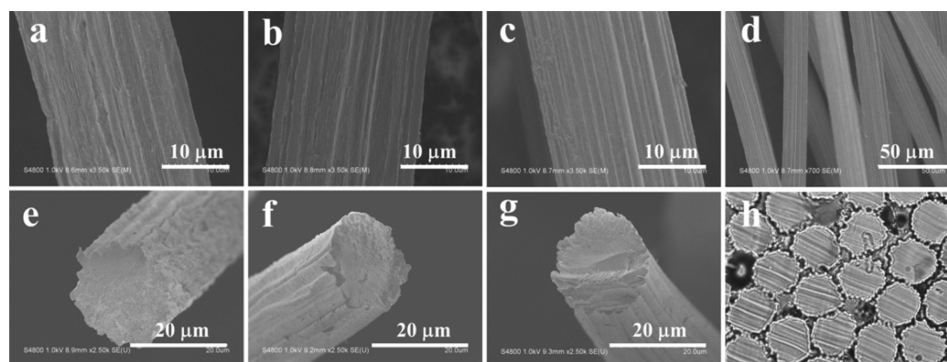


Figure 2. SEM images of the surface (top) and cross section (bottom) of the RC filaments picked up at (a, e) Nelson-type roller I (RCF-4-I), (b, f) Nelson-type roller II (RCF-4-II), and (c, g) take-up roller (RCF-4). A bundle of the RCF-4 filaments was observed by using (d) SEM and (h) optical microscopy.

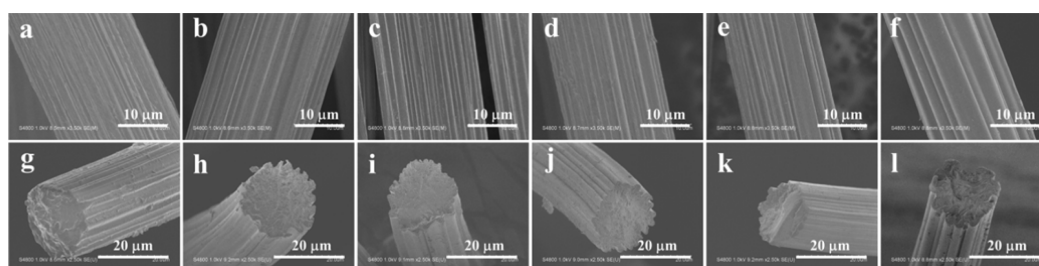


Figure 3. SEM images of the surface (top) and cross section (bottom) of the RC multifilament: (a, g) RCF-1, (b, h) RCF-2, (c, i) RCF-3, (d, j) RCF-4, (e, k) RCF-5, and (f, l) commercial viscose rayon.

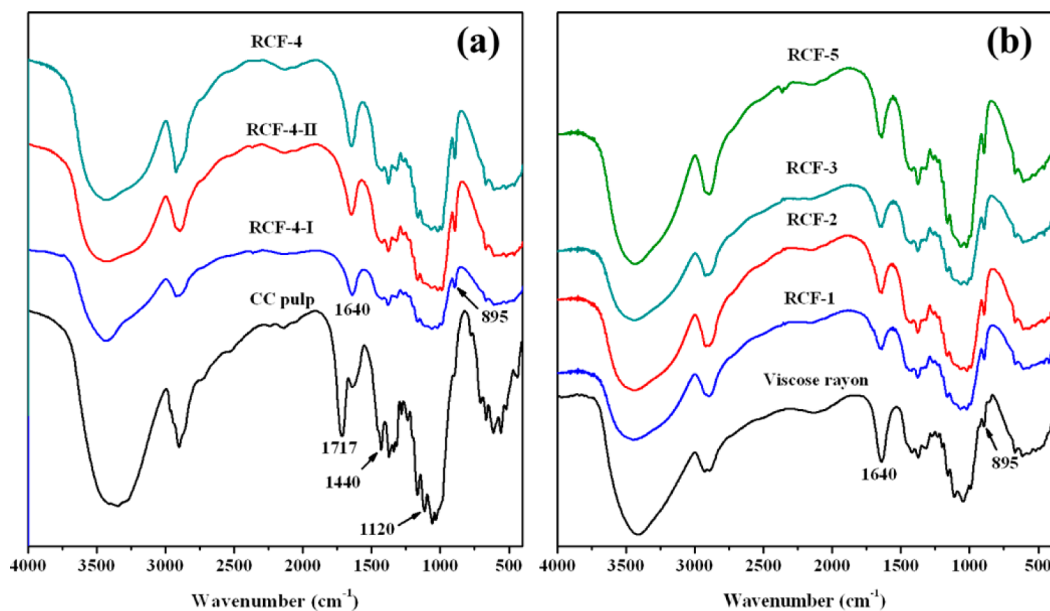


Figure 4. FTIR spectra of the RC filaments, CC pulp, and viscose rayon.

novel fibers showed good flexibility and a silk-like luster in their appearance. The sulfate content of the fibers was determined as essentially zero, whereas viscose rayon contained approximately 8 mg/100 g of multifilament. As shown in Figure 2, SEM images were obtained of the surfaces and cross sections of the RC fibers from the subsequent stages of the Nelson-type rollers I and II and take-up device. RC filaments obtained from each spinning stage displayed the same quasi-circular cross sections (Figure 2e–g). Optical microscopy analysis also presented homogeneous and cross-sectional shapes in the novel fibers

(Figure 2h), which were significantly different from the lobed-shaped and skin-core-like morphology of viscose rayon but comparable to the Lyocell fibers⁷ and cuprammonium rayon.³⁷ As shown in Figure 2a, the newly shaped RC fibers exhibited an irregular shrink structure in the surface with small voids in pore size from 40 to 240 nm. After the drawing, washing, plasticization, and drying processes in the post-processing spinning steps, the small voids on the surface gradually disappeared, and the cellulose multifilament from the take-up device exhibited a much denser structure (Figure 2c). The

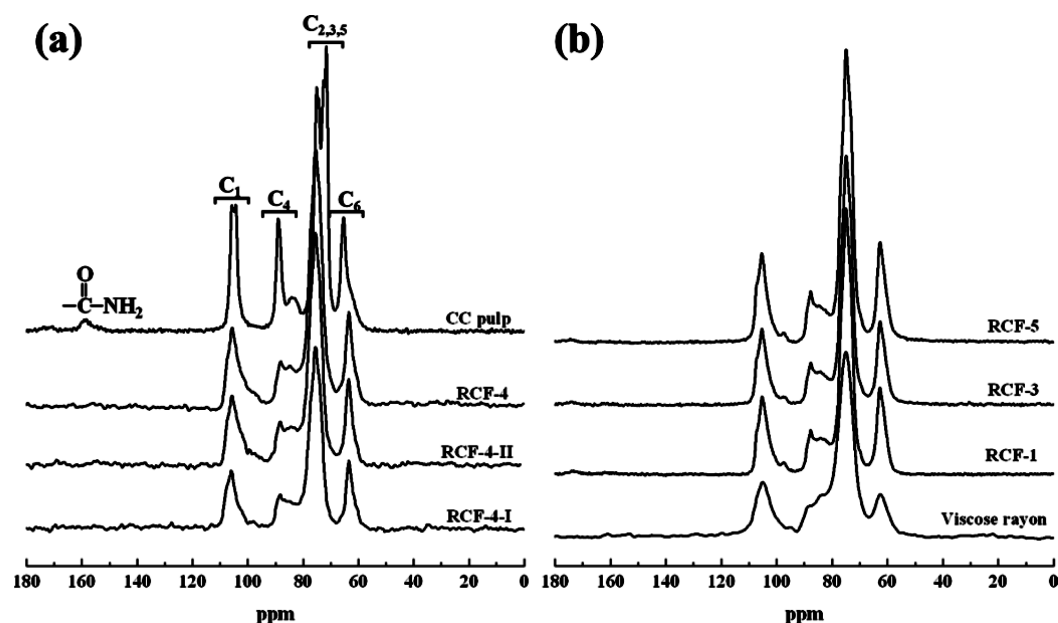


Figure 5. CP/MAS solid-state ^{13}C NMR spectra of the RC filaments, CC pulp, and viscose rayon.

coagulation of the CC spinning dope followed the well-known principles of phase separation. Lamellar cellulose almost immediately formed after the CC dope was extruded into the acidic bath.³⁸ Fibrillar cellulose was eventually regenerated as the coagulation continued, demonstrating a porous structure filled with void water. Following stretching on the Nelson-type rollers and water evaporation on the heating roller, the newly formed fiber showed a fibrilla orientation along the fiber axis and exhibited a much denser structure. The results indicated that the staged spinning process played an important role in obtaining improved structure RC fibers.

In previous reports, improved properties have been obtained in polymer fibers by increasing the drawing ratio during the spinning process.^{15,19} As shown in Figure 3, SEM images of the surface (top) and cross section (bottom) of the novel RC multifilament under different drawing ratios were compared with commercial viscose rayon. An increase in the drawing ratio from 0.50 to 0.82 produced a decrease in the diameter of the novel RC fibers from 25 to 19 μm , while still maintaining the original circular shape. The cross section of viscose rayon exhibited a lobulate shape and contained obvious pores and voids in the internal sections (Figure 3l). Meanwhile, the novel fibers exhibited a small amount of shrink structure in the surface (Figure 3a–e) and a loosely developed serrated shape, which was significantly less developed compared to the regular viscose rayon (Figure 3f). The structural differences between the fibers could be attributed to the transition process of the spinning solution into rayon. The viscose rayon transition incorporated an acid–alkali neutralization and a reversal of the xanthation reaction, which resulted in lobed-shaped and skin-core-like morphology.⁷ However, the substituent of CC was very low (0.26) compared with that of cellulose xanthogenate (about 1.57–1.90).³ The transition of cellulose in a CC–NaOH/ZnO aqueous solution was determined as a predominantly physical sol–gel process.

Structure of RC Filaments. FT-IR spectra for CC and RC filaments obtained at each spinning stage are shown in Figure 4a. The absorption band at 1430 cm^{-1} in RC was weakened and shifted to lower wavenumbers compared to the 1440 cm^{-1}

peak for CC, which was ascribed to CH_2 scissoring motion, indicating the destruction of the intramolecular hydrogen bond involving O6.³⁹ Furthermore, the band at 895 cm^{-1} in RC, characterizing the amorphous regions of cellulose, shifted to lower wavenumbers and combined with an absorbance increment when compared to CC. Moreover, a strong band was presented at 1120 cm^{-1} in the spectrum of CC, while this band was barely discernible in the RC filaments. In previous work, a relatively strong band was presented at 1120 cm^{-1} in the spectrum of cellulose I but appeared only as a shoulder in cellulose II.³⁹ Thus, the result suggested that CC completely dissolved in NaOH/ZnO aqueous solution and changed into cellulose II. The spectra of the RC filaments spun with an increased drawing ratio (Figure 4b) was similar to that of viscose rayon with cellulose II structure.³⁹ This further verified the cellulose II structure of the novel RC filaments. Particularly, the remarkable absorption peak at 1717 cm^{-1} , assigned to the stretching vibration of the carbonyl ($\text{C}=\text{O}$),⁴⁰ disappeared completely in the spectra of RC fibers (Figure 4a and b). Moreover, the nitrogen content of the multifilament fibers was determined as essentially zero. The results indicated that the carbamate groups were successfully cleaved off from the cellulose backbone through a one-step coagulation process. In contrast with the conventional carbamate process, the final alkaline bath for substituent removal was unnecessary in our new process. This novel carbamate process was thus simpler and more economical.

Figure 5a shows the CP/MAS ^{13}C NMR spectra of the RC fibers collected at different spinning stages in addition to the CC sample. The spectra of the RC multifilament exhibited four main peaks at 105.8, 88.0, 75.6, and 63.4 ppm assigned to the C1, C4, C2,3,5 and C6, respectively. The C6 peak for the CC pulp was located at 65.4 ppm, while the C6 peak for the novel fibers showed a shift to a higher magnetic field at 63.4 ppm, suggesting that the “t-g” conformation of the C6–OH group (for cellulose I) transformed into a “g-t” conformation (for the family II cellulose) and simultaneously formed the intramolecular hydrogen bonds $\text{O6-H}\cdots\text{O}_2'$.⁴¹ The results confirmed the transformation of the CC dope into cellulose

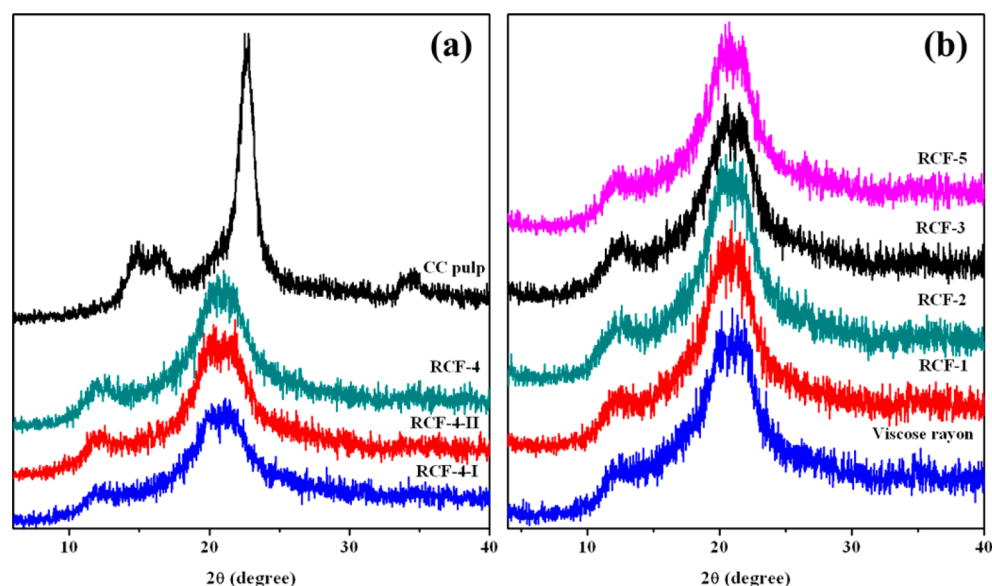


Figure 6. XRD patterns of the RC filaments, CC pulp, and viscose rayon.

Table 2. Physical Properties of Novel RC Filaments Compared with Viscose Rayon

sample	DP	χ_c (%)	Π (%)	f	tenacity (cN/dtex)		elongation (%)		fineness (denier)	K/S value
					σ_b , dry	σ_b , wet	ϵ_b , dry	ϵ_b , wet		
RCF-1	550	54	83	0.85	1.69	0.61	21.2	24.9	7.8	51
RCF-2	550	54	83	0.85	1.92	0.69	16.2	21.4	6.9	51
RCF-3	550	56	84	0.86	2.11	0.71	15.9	18.7	5.2	50
RCF-4-I	550	50	77	0.81	1.44	0.40	25.3	26.3	5.4	53
RCF-4-II	550	53	80	0.83	1.63	0.58	21.5	23.5	5.2	51
RCF-4	550	56	85	0.87	2.36	0.73	15.9	17.8	5.1	50
RCF-5	550	57	85	0.87	2.31	0.79	14.8	18.7	5.0	50
viscose rayon	371	50	84	0.86	2.11	1.22	19.8	26.2	4.9	48

DP, degree of polymerization; χ_c , degree of crystallinity; Π , degree of orientation; f , Hermans' orientation parameter; and K/S, color strength

II after the gel was regenerated in the coagulation bath. In the RCF-4-I, RCF-4-II, and RCF-4 multifilament, the C4 peaks located at 88.0 ppm shifted to higher magnetic fields than the CC pulp (89.0 ppm), and the intensity was significantly lower. This result suggested a decrease in crystallinity as a result of the regeneration of cellulose molecules from the coagulation process.⁴² A previous study found that the appearance of the C4 signal at around 88.0 ppm in RC fibers and its shoulder peak at 84.6 ppm was dependent on the status of the carbon in the crystalline or amorphous regions, respectively. It was supposed that the C4 shoulder peak at 84 ppm in the RC fibers could be related to the degree of anisotropy. There was an evident increase in the C4 shoulder in the RC filaments from RCF-4-I to RCF-4, reflecting an increase in the degree of anisotropy or more specifically, an increase in chain orientation. There was a clear difference between the RC fibers and CC samples in the appearance of the carbonyl carbon signal at 158.6 ppm,^{29,30} which indicated that the carbamate groups were successfully cleaved off from the cellulose backbone after coagulation in the acid bath. The ¹³C NMR spectra of viscose rayon and cuprammonium rayon indicated higher orientation with drawing.²⁰ As shown in Figure 5b, the CP/MAS ¹³C NMR spectra of the novel RC filaments spun from different drawing ratios showed very similar cellulose II structure to that of viscose rayon. Furthermore, broad shielding shoulders appeared in the C4 regions of the novel fibers (RCF-1). In a comparison

of the ¹³C NMR spectrum of RCF-1, the C4 peak of the fibers (RCF-3 and RCF-5) was narrower, indicating better chain orientation. A signal for carbonyl carbon did not appear in any of the spectra for the three RC fibers. This suggested that the structure of RC fibers could be improved with the optimization of the spinning conditions and further indicated the removal of carbamate groups below the lower detection limit of NMR during the coagulation process.

Figure 6a shows the XRD patterns of CC and RC fibers at different spinning stages. The crystalline form of CC typically has diffraction peaks at $2\theta = 14.6^\circ$, 16.3° , and 22.6° . However, the RC fibers obtained on the Nelson-type rollers I and II and take-up roller showed new broad peaks at $2\theta = 12.2^\circ$, 20.2° , and 21.9° , which were assigned to the (1 $\bar{1}$ 0), (110), and (020) planes of the cellulose II crystalline form, respectively.⁴³ This also suggested that a conversion from cellulose I (CC pulp) to cellulose II (RC fiber) had occurred. The χ_c values calculated from the XRD patterns for the RC fibers are listed in Table 2. The χ_c values of CC pulp (64%) decreased when compared to the native cellulose (71%) with an introduction of carbamate group. Moreover, slightly increased χ_c values were observed in the RC fibers with the spinning process, indicating a relatively denser structure. As shown in Figure 6b and Table 2, the drawing ratio also influenced the crystal structure of the RC fibers. As the drawing ratio increased from 0.50 to 0.82, the χ_c value increased from 54% to 57%, which was higher than

viscose rayon (50%) and comparable with Lyocell fiber (55%).⁷ These results were generally in accordance with the previous report.⁷

Figure 7 shows the 2D WAXD patterns of the RC fibers in addition to viscose rayon and Lyocell fibers. All of the RC fibers

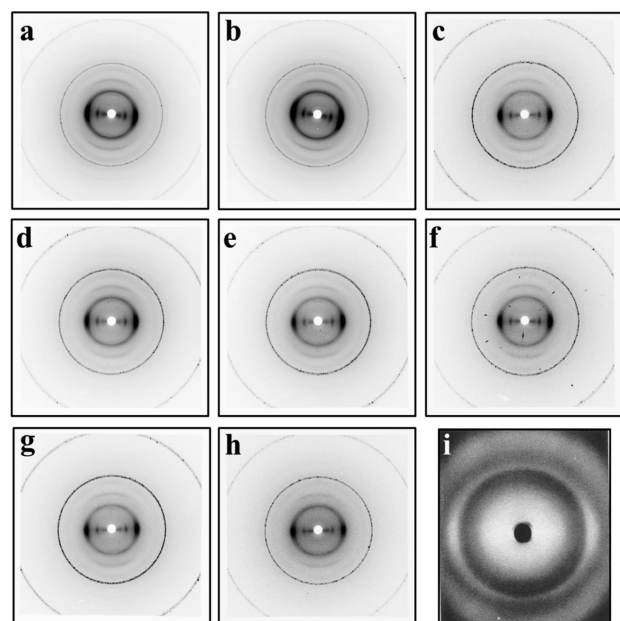


Figure 7. 2D WAXD patterns of the RC filaments: (a) RCF-4-I, (b) RCF-4-II, (c) RCF-4, (d) RCF-1, (e) RCF-2, (f) RCF-3, and (g) RCF-5, together with (h) commercial viscose rayon and (i) Lyocell fiber.⁷

exhibited a cellulose II structure.¹⁹ It was thus confirmed that the dissolution processes could generate cellulose II similar to that produced in the viscose process and NMMO system. The WAXD patterns of RCF-4-I and RCF-4-II showed strong similarities, and their reflections all appeared as broad arcs, indicating moderate crystal orientation. However, the WAXD pattern reflections of RC-4 collected on the take-up roller exhibited narrow equatorial arcs, which suggested a high degree of crystal orientation. RC fibers spun with an increased drawing ratio all presented in narrow equatorial arc patterns, similar to those in viscose and Lyocell fibers.^{7,19} As shown in Table 2, the degree of orientation and Hermans' orientation parameter for the RC fibers increased with improved post-treatment spinning steps, particularly after the heating process. Increased drawing ratio on the Nelson-type roller I provided slightly increased orientation in the RC fibers collected at the take-up roller in the ranges of 83–85% and 0.85–0.87, respectively. Moreover, the RC fibers (RCF-4 and RCF-5) obtained at higher spinning speed demonstrated higher Hermans' orientation parameters than that of commercial viscose rayon with levels comparable to Lyocell and Ionicell fibers.¹³ It was thus determined that the post-processing spinning steps and drawing process could be redesigned to improve the final cellulose structure.

Physiochemical Properties. The tenacity (σ_b) and elongation at break (ϵ_b) of the novel fibers and the commercial viscose rayon are summarized in Table 2. During the post-processing spinning steps, a dramatic increase was observed in the tenacity of the RC fibers in the dry state, while the elongation at break decreased. This could be attributed to an increasingly dense structure in RCF-4-I to RCF-4. Moreover, tenacity increased with increased drawing ratio, while the value (2.31–2.36 cN/dtex) obtained at high spinning speed was

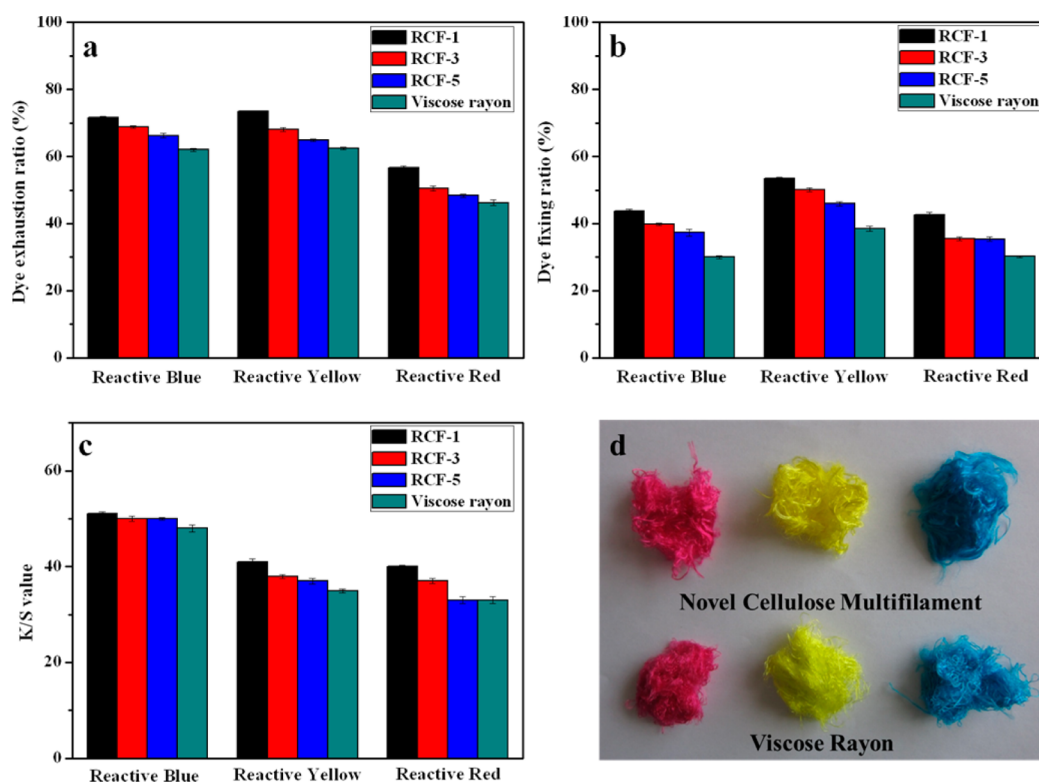


Figure 8. Comparison of the dyeing properties of the RC multifilament and viscose rayon: (a) dye exhaustion ratio, (b) dye fixing ratio, and (c) K/S value. (d) Photograph of the dyed yarns from the RC multifilament and viscose rayon.

higher than that of the commercial viscose rayon (2.11 cN/dtex). The higher tenacity in the obtained RC fibers, as compared to viscose rayon, could be ascribed to higher crystallinity and degree of orientation. It was noted that the tenacity of the RC fibers showed no obvious change in wet state under changed spinning conditions and were obtained in the range of 0.61–0.79 cN/dtex. The values were achieved in the range of the National Standards of China (GBT13758-2008) for cellulose filaments (0.75 cN/dtex), although they were lower than the value of viscose rayon. It was anticipated that the mechanical properties of the fibers could be improved after further optimization of the spinning process, particularly with enhancements to the coagulation bath. The obtained cellulose filaments had a higher DP than that of viscose rayon (DP = 371). The shrinkage in boiling water of the RC fibers was in the range of 6.0–6.2%. Meanwhile, the linear density of the RC fibers decreased from 7.8 to 5.0 denier with increased spinning speed, and moisture recovery levels reached 13.33%. Similar values were observed in silk fibers, with denier in the range of 2.3–10.7 and moisture recovery at 6.70–12.05%, which signified good wearable comfort and structural stability.^{44,45} As illustrated in Scheme 1, the described method was advantageous in requiring just one coagulant bath when compared with the conventional viscose process, while avoiding the release of toxic gas during coagulation. Moreover, there were neither organic transfer mediums (xylene) nor catalytic agents (sodium carbonate) used, and the energy savings was over 50% when compared to the conventional synthesis of CC.³¹ Furthermore, the ZnO could be well recovered from the coagulation bath and washing water by adding CaO through the two-step precipitation method.⁴⁶ Therefore, the novel carbamate process demonstrated great potential for the production of high-quality cellulose multifilament in a much more environmentally friendly and economic way, in addition to potential for applications in the development of viscose-like products.

High-quality dye properties and color strength are very significant for wider application in the textile industry. The dye properties of the RC fibers were estimated using the dye exhaustion ratio, dye fixing ratio, and K/S values (Figure 8), and the subsequent results were compared with commercial viscose rayon. As shown in Figure 8a, the dye exhaustion ratio of the RC fibers decreased with increased drawing ratio in the three dyes. This was attributed to higher crystallinity and degree of orientation at high spinning speed. The dye exhaustion ratio was higher in the RC fibers than in viscose rayon, although they also possessed higher orientation, which was most likely due to their different structure. As presented in Figure 3, our novel RC fiber had a homogeneous structure. However, viscose rayon consistently presented a large surface skin region due to the occurrence of a bychemical reaction. This denser skin layer may have impeded the diffusion of the dyes. Moreover, the dye exhaustion ratio of the RC fibers was higher with the reactive yellow dye than with the reactive blue and reactive red dyes. This could be attributed to the shape of the dye molecules and the interaction between the dye and cellulose molecules.¹¹ All three dyes showed higher dye fixing ratios in the RC fibers than in viscose rayon (Figure 8b). These results established the suitability of reactive dyes for use with RC fibers, as with commercial viscose rayon. Figure 8c and Table 2 compare the K/S values in the novel RC fibers and viscose rayon. Higher K/S values correlated with brighter color in the dyed fibers.¹¹ The K/S values for reactive blue in the RC

fibers were within the range of 50–53, which was significantly higher than in viscose rayon (48), Ionicell (~20) and Lyocell fibers (~9).¹¹ Moreover, the overall K/S values for the three reactive dyes were higher in the RC fibers than in viscose rayon. The novel RC fibers had excellent dye properties, which displayed brighter color than viscose rayon (Figure 8d). The result is in accordance with the high dye uptake reported for CarbaCell fibers.⁵

CONCLUSIONS

In summary, novel nitrogen- and sulfur-free RC filaments were successfully spun on an extended laboratory scale from CC–NaOH/ZnO dope via a pilot machine using a one-step acid coagulation process. The CC transition in NaOH/ZnO solution was determined as a predominantly physical sol–gel process. The fibers exhibited cellulose II characteristics and displayed a circular cross section with a homogeneous structure. Following multidrawing and drying processes, the small voids on the surface of the fibers gradually disappeared, and a much denser structure was shown in the fibers from the take-up device. An increased drawing ratio provided improved tenacity and degree of orientation in the fibers, reaching 2.36 cN/dtex and 85%, respectively. Furthermore, RC filaments demonstrated excellent dye properties with different reactive dyes, K/S values were determined in the range of 50–53 for the reactive blue dye. The new pathway was intentionally similar to existing viscose systems, therefore allowing for cost-effective implementation in industry. This simple and environmentally friendly approach offered great potential for application in the production of cellulose fibers, films, nonwoven fabrics, and functional materials on an industrial scale.

AUTHOR INFORMATION

Corresponding Author

*Fax: (+) 86-27-68754067. E-mail: zhoujp325@whu.edu.cn.

Notes

The authors declare no competing financial interest.

ACKNOWLEDGMENTS

This work was financially supported by the National Natural Science Foundation of China (51273151), Program for New Century Excellent Talents in University (NCET-11-0415), and Natural Science Foundation of Hubei Province (2009CDA040).

REFERENCES

- (1) Håkansson, K. M.; Fall, A. B.; Lundell, F.; Yu, S.; Krywka, C.; Roth, S. V.; Santoro, G.; Kvik, M.; Wittberg, L. P.; Wågberg, L.; Söderberg, L. D. Hydrodynamic alignment and assembly of nanofibrils resulting in strong cellulose filaments. *Nature Commun.* **2014**, *5*, 4018.
- (2) Guo, B.; Chen, W.; Yan, L. Preparation of flexible, highly transparent, cross-linked cellulose thin film with high mechanical strength and low coefficient of thermal expansion. *ACS Sustainable Chem. Eng.* **2013**, *1*, 1474–1479.
- (3) Klemm, D.; Heublein, B.; Fink, H. P.; Bohn, A. Cellulose: Fascinating biopolymer and sustainable raw material. *Angew. Chem., Int. Ed.* **2005**, *44*, 3358–3393.
- (4) Qi, H.; Liu, J.; Gao, S.; Mäder, E. Multifunctional films composed of carbon nanotubes and cellulose regenerated from alkaline–urea solution. *J. Mater. Chem. A* **2013**, *1*, 2161–2168.
- (5) Fink, H. P.; Ganster, J.; Lehmann, A. Progress in cellulose shaping: 20 years industrial case studies at Fraunhofer IAP. *Cellulose* **2014**, *21*, 31–51.

- (6) Cai, J.; Zhang, L.; Zhou, J.; Qi, H.; Chen, H.; Kondo, T.; Chen, X.; Chu, B. Multifilament fibers based on dissolution of cellulose in NaOH/urea aqueous solution: Structure and properties. *Adv. Mater.* **2007**, *19*, 821–825.
- (7) Fink, H. P.; Weigel, P.; Purz, H. J.; Ganster, J. Structure formation of regenerated cellulose materials from NMMO-solutions. *Prog. Polym. Sci.* **2001**, *26*, 1473–1524.
- (8) Gao, Q.; Shen, X.; Lu, X. Regenerated bacterial cellulose fibers prepared by the NMMO-H₂O process. *Carbohydr. Polym.* **2011**, *83*, 1253–1256.
- (9) Swatloski, R. P.; Spear, S. K.; Holbrey, J. D.; Rogers, R. D. Dissolution of cellulose with ionic liquids. *J. Am. Chem. Soc.* **2002**, *124*, 4974–4975.
- (10) Zhang, H.; Wu, J.; Zhang, J.; He, J. 1-Allyl-3-methylimidazolium chloride room temperature ionic liquid: A new and powerful nonderivatizing solvent for cellulose. *Macromolecules* **2005**, *38*, 8272–8277.
- (11) Cai, T.; Zhang, H.; Guo, Q.; Shao, H.; Hu, X. Structure and properties of cellulose fibers from ionic liquids. *J. Appl. Polym. Sci.* **2010**, *115*, 1047–1053.
- (12) Zhang, H.; Wang, Z.; Zhang, Z.; Wu, J.; Zhang, J.; He, J. Regenerated-cellulose/multiwalled-carbon-nanotube composite fibers with enhanced mechanical properties prepared with the ionic liquid 1-allyl-3-methylimidazolium chloride. *Adv. Mater.* **2007**, *19*, 698–704.
- (13) Jiang, G.; Huang, W.; Li, L.; Wang, X.; Pang, F.; Zhang, Y.; Wang, H. Structure and properties of regenerated cellulose fibers from different technology processes. *Carbohydr. Polym.* **2012**, *87*, 2012–2018.
- (14) Kosan, B.; Michels, C.; Meister, F. Dissolution and forming of cellulose with ionic liquids. *Cellulose* **2008**, *15*, 59–66.
- (15) Cai, J.; Zhang, L. Rapid dissolution of cellulose in LiOH/urea and NaOH/urea aqueous solutions. *Macromol. Biosci.* **2005**, *5*, 539–548.
- (16) Zhang, L.; Ruan, D.; Gao, S. Dissolution and regeneration of cellulose in NaOH/thiourea aqueous solution. *J. Polym. Sci., Part B: Polym. Phys.* **2002**, *40*, 1521–1529.
- (17) Sen, S.; Martin, J. D.; Argyropoulos, D. S. Review of cellulose non-derivatizing solvent interactions with emphasis on activity in inorganic molten salt hydrates. *ACS Sustainable Chem. Eng.* **2013**, *1*, 858–870.
- (18) Ruan, D.; Zhang, L.; Lue, A.; Zhou, J.; Chen, H.; Chen, X.; Chu, B.; Kondo, T. A rapid process for producing cellulose multi-filament fibers from a NaOH/thiourea solvent system. *Macromol. Rapid Commun.* **2006**, *27*, 1495–1500.
- (19) Chen, X.; Burger, C.; Fang, D.; Ruan, D.; Zhang, L.; Hsiao, B. S.; Chu, B. X-ray studies of regenerated cellulose fibers wet spun from cotton linter pulp in NaOH/thiourea aqueous solutions. *Polymer* **2006**, *47*, 2839–2848.
- (20) Cai, J.; Zhang, L.; Zhou, J.; Li, H.; Chen, H.; Jin, H. Novel fibers prepared from cellulose in NaOH/urea aqueous solution. *Macromol. Rapid Commun.* **2004**, *25*, 1558–1562.
- (21) Li, R.; Chang, C.; Zhou, J.; Zhang, L.; Gu, W.; Li, C.; Liu, S.; Kuga, S. Primarily industrialized trial of novel fibers spun from cellulose dope in NaOH/urea aqueous solution. *Ind. Eng. Chem. Res.* **2010**, *49*, 11380–11384.
- (22) Yan, L.; Qi, X. Degradation of cellulose to organic acids in its homogeneous alkaline aqueous solution. *ACS Sustainable Chem. Eng.* **2014**, *2*, 897–901.
- (23) Woodings, C. *Regenerated Cellulose Fibres*; Woodhead Publishing: Cambridge, U.K., 2001.
- (24) Rose, M.; Palkovits, R. Cellulose-based sustainable polymers: State of the art and future trends. *Macromol. Rapid Commun.* **2011**, *32*, 1299–1311.
- (25) Labafzadeh, S. R.; Kavakka, J. S.; Vyavaharkar, K.; Sievänen, K.; Kilpeläinen, I. Preparation of cellulose and pulp carbamates through a reactive dissolution approach. *RSC Adv.* **2014**, *4*, 22434–22441.
- (26) Yin, C.; Shen, X. Synthesis of cellulose carbamate by supercritical CO₂-assisted impregnation: Structure and rheological properties. *Eur. Polym. J.* **2007**, *43*, 2111–2116.
- (27) Mormann, W.; Michel, U. Improved synthesis of cellulose carbamates without by-products. *Carbohydr. Polym.* **2002**, *50*, 201–208.
- (28) Guo, Y.; Zhou, J.; Zhang, L. Dynamic viscoelastic properties of cellulose carbamate dissolved in NaOH aqueous solution. *Biomacromolecules* **2011**, *12*, 1927–1934.
- (29) Guo, Y.; Zhou, J.; Song, Y.; Zhang, L. An efficient and environmentally friendly method for the synthesis of cellulose carbamate by microwave heating. *Macromol. Rapid Commun.* **2009**, *30*, 1504–1508.
- (30) Guo, Y.; Zhou, J.; Wang, Y.; Zhang, L.; Lin, X. An efficient transformation of cellulose into cellulose carbamates assisted by microwave irradiation. *Cellulose* **2010**, *17*, 1115–1125.
- (31) Fu, F.; Zhou, J.; Zhou, X.; Zhang, L.; Li, D.; Kondo, T. Green method for the production of cellulose multifilament from cellulose carbamate on a pilot-scale. *ACS Sustainable Chem. Eng.* **2014**, DOI: 10.1021/sc5003787.
- (32) Fu, F.; Guo, Y.; Wang, Y.; Tan, Q.; Zhou, J.; Zhang, L. Structure and properties of the regenerated cellulose membranes prepared from cellulose carbamate in NaOH/ZnO aqueous solution. *Cellulose* **2014**, *212*, 819–830.
- (33) Brown, W.; Wikström, R. A viscosity-molecular weight relationship for cellulose in cadoxen and a hydrodynamic interpretation. *Eur. Polym. J.* **1965**, *1*, 1–10.
- (34) Yu, L.; Lin, J.; Tian, F.; Li, X.; Bian, F.; Wang, J. Cellulose nanofibrils generated from jute fibers with tunable polymorphs and crystallinity. *J. Mater. Chem. A* **2014**, *2*, 6402–6411.
- (35) Sehaqui, H.; Ezekiel Mushi, N.; Morimune, S.; Salajkova, M.; Nishino, T.; Berglund, L. A. Cellulose nanofiber orientation in nanopaper and nanocomposites by cold drawing. *ACS Appl. Mater. Interfaces* **2012**, *4*, 1043–1049.
- (36) GBT13758-2008: The National Standard for Viscose Filament Yarn (in Chinese), China Standard: Beijing, 2005.
- (37) Woodings, C. R. The development of advanced cellulosic fibres. *Int. J. Biol. Macromol.* **1995**, *17*, 305–309.
- (38) Altena, F. W.; Smolders, C. A. Calculation of liquid–liquid phase separation in a ternary system of a polymer in a mixture of a solvent and a nonsolvent. *Macromolecules* **1982**, *15*, 1491–1497.
- (39) Carrillo, F.; Colom, X.; Sunol, J. J.; Saurina, J. Structural FTIR analysis and thermal characterisation of lyocell and viscose-type fibres. *Eur. Polym. J.* **2004**, *40*, 2229–2234.
- (40) Nada, A. M. A.; Hassan, M. L. Thermal behavior of cellulose and some cellulose derivatives. *Polym. Degrad. Stab.* **2000**, *67*, 111–115.
- (41) Casas, A.; Alonso, M. V.; Olliet, M.; Santos, T. M.; Rodriguez, F. Characterization of cellulose regenerated from solutions of pine and eucalyptus woods in 1-allyl-3-methylimidazolium chloride. *Carbohydr. Polym.* **2013**, *92*, 1946–1952.
- (42) Cuculo, J. A.; Smith, C. B.; Sangwatanaroj, U.; Stejskal, E. O.; Sankar, S. S. A study on the mechanism of dissolution of the cellulose/NH₃/NH₄SCN system. *J. Polym. Sci. Part A: Polym. Chem.* **1994**, *32*, 229–239.
- (43) Chen, M.; Zhang, X.; Liu, C.; Sun, R.; Lu, F. Approach to renewable lignocellulosic biomass film directly from bagasse. *ACS Sustainable Chem. Eng.* **2014**, *2*, 1164–1168.
- (44) Reddy, N.; Yang, Y. Structure and properties of ultrafine silk fibers produced by *Theriodopteryx ephemeraeformis*. *J. Mater. Sci.* **2010**, *45*, 6617–6622.
- (45) Maji, T. K.; Basu, D.; Datta, C.; Banerjee, A. Studies of mechanical and moisture regain properties of methyl methacrylate grafted silk fibers. *J. Appl. Polym. Sci.* **2002**, *84*, 969–974.
- (46) Wang, K.; Liu, J.; Lu, Y.; Gao, B. Method for Recovering Zinc from Zinc Sulfate Solution. China Patent CN101760632 (A), 2008.